A Discrete and Discontinuous Increase in Micellar Aggregation Number: Effects of Alkyl Chain Length on Platonic Micelles

Shota Fujii[†]*, Shimpei Yamada*[†]*, Masataka Araki, Ji Ha Lee, Rintaro Takahashi, and Kazuo Sakurai**

Department of Chemistry and Biochemistry, University of Kitakyushu, 1-1 Hibikino, Kitakyushu, Fukuoka 808-0135, Japan

[†]These authors contributed equally to this work.

*Corresponding authour

Table of Contents

General considerations

Materials and Synthesis. All chemical reagents were purchased from Tokyo Chemical Industry Co. and Sigma-Aldrich Co., which were used without further purification. The chemical reactions for the synthesis of quaternary amines bearing calix[4]arene-based amphiphiles was carried out under nitrogen atmosphere. The progress of the reactions was monitored using thin layer chromatography (TLC), and detected using ultraviolet (UV; 254 nm) irradiation. Nuclear magnetic resonance spectra were recorded with a 500 MHz Bruker spectrometer using methanol-d4 as solvents.

Synthesis procedures of quaternary amines bearing calix[4]arene-based amphiphiles

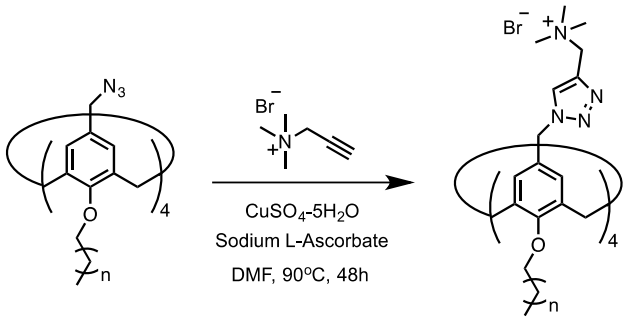

Synthesis of quaternary amines bearing calix[4]arene lipid with propyl tails (QACaL3). N,N,N-trimethyl-2-propyn-1-ammmonium bromide (0.280 g, 1.57 mmol), copper(II) sulfate pentahydrate (4.10 mg, 16.4 μmol), and sodium ascorbate (32.1 mg, 0.162 mmol) were dissolved in dry DMF (10 mL), and then a solution of azide bearing calix[4]arene derivative (0.127 g, 0.156 mmol) in dry DMF (5 mL) was added to the mixture. The reaction mixture was stirred for 48 h at 90 °C. The mixture was cooled to room temperature, and then concentrated at reduced pressure. The crude product was purified by reversed phase silica gel column chromatography (water), which afforded a brown solid (0.1863 g, 0.121 mol, 76%). ^{1}H NMR (500 MHz, methanol-d4): δ (ppm) = 8.46 (s, 4H), 6.71 (s, 8H), 5.40 (s, 8H), 4.75 (s, 8H), 4.46 (d, J = 10.0 Hz, 4H), 3.83 (t, J = 7.50 Hz, 8H), 3.21 (d, 4H), 3.17 (s, 9H), 1.90 (m, 8H), 1.00 (t, J = 7.5 Hz 12H). ESI–MS (M^{2+}/2): calcd for $C_{68}H_{100}Br_2N_{16}O_4$ 682.32, found 682.34.

Synthesis of quaternary amines bearing calix[4]arene lipid with butyl tails (QACaL4). QACaL4 was synthesized using a similar procedure described for QACaL3. Yield: 0.168 g, 0.107 mol, 20%. ^{1}H NMR (500 MHz, methanol-d4): δ (ppm) = 8.41 (s, 4H), 6.69 (s, 8H), 5.37 (s, 8H), 4.68 (s, 8H), 4.38 (d, J = 10.0 Hz, 4H),

3.62 (t, *J* = 7.50 Hz, 8H), 3.17 (d, 4H), 3.09 (s, 9H), 1.83 (m, 8H), 1.42 (m, 8H), 0.94 (t, *J* = 7.5 Hz 12H). ESI–MS ($M^{2+}/2$): calcd for $C_{72}H_{108}Br_2N_{16}O_4$ 710.35, found 710.37.

Synthesis of quaternary amines bearing calix[4]arene lipid with pentyl tails (QACaL5). QACaL5 was synthesized using a similar procedure described for QACaL3. Yield: 0.631 g, 0.386 mol, 93%. ^{1}H NMR (500 MHz, methanol-d4): δ (ppm) = 8.38 (s, 4H), 6.65 (s, 8H), 5.34 (s, 8H), 4.68 (s, 8H), 4.37 (d, *J* = 10.0 Hz, 4H), 3.61 (t, *J* = 7.50 Hz, 8H), 3.16 (d, 4H), 3.09 (s, 9H), 1.84 (m, 8H), 1.35 (m, 8H), 0.89 (t, *J* = 7.5 Hz 12H). ESI–MS ($M^{2+}/2$): calcd for $C_{76}H_{116}Br_2N_{16}O_4$ 738.39, found 738.41.

Synthesis of quaternary amines bearing calix[4]arene lipid with hexyl tails (QACaL6). QACaL6 was synthesized using a similar procedure described for QACaL3. Yield: 0.241 g, 0.142 mol, 80%. ^{1}H NMR (500 MHz, methanol-d4): δ (ppm) = 8.47 (s, 4H), 6.73 (s, 8H), 5.41 (s, 8H), 4.75 (s, 8H), 4.43 (d, *J* = 10.0 Hz, 4H), 3.87 (t, *J* = 7.50 Hz, 8H), 3.17 (d, 4H), 3.16 (s, 9H), 1.91 (m, 8H), 1.38 (m, 8H), 0.94 (t, *J* = 7.5 Hz 12H). ESI–MS ($M^{2+}/2$): calcd for $C_{80}H_{124}Br_2N_{16}O_4$ 766.42, found 766.44.

Synthesis of quaternary amines bearing calix[4]arene lipid with heptyl tails (QACaL7). QACaL7 was synthesized using a similar procedure described for QACaL3. Yield: 0.123 g, 0.0705 mol, 86%. ^{1}H NMR (500 MHz, methanol-d4): δ (ppm) = 8.48 (s, 4H), 6.71 (s, 8H), 5.40 (s, 8H), 4.78 (s, 8H), 4.43 (d, *J* = 15.0 Hz, 4H), 3.87 (t, *J* = 7.50 Hz, 8H), 3.24 (d, 4H), 3.19 (s, 9H), 1.91 (m, 8H), 1.35 (m, 8H), 0.91 (t, *J* = 7.5 Hz 12H). ESI–MS ($M^{2+}/2$): calcd for $C_{84}H_{132}Br_2N_{16}O_4$ 794.45, found 794.47.

Synthesis of quaternary amines bearing calix[4]arene lipid with octyl tails (QACaL8). QACaL8 was synthesized using a similar procedure described for QACaL3. Yield: 0.113 g, 0.0626 mmol, 68%. ^{1}H NMR (500 MHz, methanol-d4): δ (ppm) = 8.45 (s, 4H), 6.71 (s, 8H), 5.40 (s, 8H), 4.76 (s, 8H), 4.43 (d, *J* = 15.0 Hz, 4H), 3.86 (t, *J* = 7.50 Hz, 8H), 3.23 (d, 4H), 3.18 (s, 9H), 1.91 (m, 8H), 1.35 (m, 8H), 0.89 (t, *J* = 7.5 Hz 12H). ESI–MS ($M^{2+}/2$): calcd for $C_{88}H_{141}Br_2N_{16}O_4$ 822.48, found 822.51.

Synthesis of quaternary amines bromides bearing calix[4]arene lipid with nonyl tails (QACaL9). QACaL9 was synthesized using a similar procedure described for QACaL3. Yield: 0.448 g, 0.241 mmol, 92%. ^{1}H NMR (500 MHz, methanol-d4$CDCl_3$): δ (ppm) = 8.43 (s, 4H), 6.72 (s, 8H), 5.41 (s, 8H), 4.75 (s, 8H), 4.43 (d, *J* = 15.0 Hz, 4H), 3.85 (t, *J* = 7.50 Hz, 8H), 3.18 (d, 4H), 3.15 (s, 9H), 1.91 (m, 8H), 1.32 (m, 8H), 0.90 (t, *J* = 7.5 Hz 12H). ESI–MS ($M^{2+}/2$): calcd for $C_{92}H_{148}Br_2N_{16}O_4$ 850.51, found 850.53.

Characterization of micellar structures with small angle scattering and analytical ultracentrifugation measurements

Small angle X-ray scattering (SAXS) measurements. The powder of QACaL*n* was dissolved in 50 mM aqueous NaCl to be required concentration. The prepared samples were left for at least one day to equilibrate at room temperature. Small angle X-ray scattering (SAXS) measurements were carried out at the BL-40B2 beamline of the SPring-8 facility, Hyōgo Prefecture, Japan. A 30 × 30 cm imaging plate (Rigaku R-AXIS VII) detector was placed 1 m from the sample. The wavelength of the incident beam (λ) was adjusted to 0.10 nm. This setup provided a q range of 0.20−4 nm^{-1}, where q is the magnitude of the scattering vector, defined as $q = 4\pi \sin\theta/\lambda$, with a scattering angle of 2θ. The X-ray transmittance of the samples was determined by using ion chambers located in front of and behind the sample. The detailed experimental procedures are reported elsewhere.[1] The absolute SAXS intensities were recorded using the absolute scattering intensities of water.[2, 3] The micellar SAXS profiles were fitted to core-shell spheres by using the following expression [4]:

$$I(q) = \left\{ 3V_{\mathrm{C}}(\rho_{\mathrm{C}} - \rho_{S}) \frac{j_1(qR_{\mathrm{C}})}{qR_{\mathrm{C}}} + 3V_{\mathrm{S}}\rho_{\mathrm{S}} \frac{j_1(qR_{\mathrm{S}})}{qR_{\mathrm{S}}} \right\}^2 \tag{1}$$

$$I(q) = \frac{L\pi}{q} \left\{ S_{\mathrm{C}}(\rho_{\mathrm{C}} - \rho_{\mathrm{S}}) \frac{J_1(qR_{\mathrm{C}})}{qR_{\mathrm{C}}} + S_{\mathrm{S}}(\rho_{\mathrm{S}} - \rho_{\mathrm{Sol}}) \frac{J_1(qR_{\mathrm{S}})}{qR_{\mathrm{S}}} \right\}^2 \tag{2}$$

Here, R_{c} and R_{s} are the outer radii of the core and micelle (core + shell), and ρ_{c}, ρ_{s}, and ρ_{sol} are the electron density of the core, the shell, and the solvent, respectively. J_1 and j_1 are the first Bessel function and second spherical Bessel function, respectively. V_{c} and V_{s} are the particle volume of the core and micelle (core + shell), respectively. S_{C} and S_{S} are the cross-sectional areas of the core and micelle (core + shell), respectively. The SAXS profiles in the low q region follow the Guinier relation given by the following equation [4]:

$$I(q) = I(0)\exp(-q^2 R_{\mathrm{g}}^{\ 2} / 3) \tag{3}$$

where $I(0)$ is the forward scattering intensity at $q = 0$. $I(0)$ and the gyration radius (R_{g}) are determined from the intercept and the slope of the $\ln(I(q))$ vs. q^2 plot (Guinier plot). Due to inter-particle interference, the $I(0)$ and R_{g} values depend on the sample concentration. In order to remove the concentration effects, the SAXS intensities recorded at different concentrations were extrapolated to zero concentration.

Determination of micellar molar mass by SAXS. The molar mass of the micelles can be given by the following equation [4]:

$$M_{\mathrm{w}} = I(0)\{N_{\mathrm{A}}\mathrm{c}(\Delta\rho\bar{\upsilon})^2\} \quad (4)$$

Where M_{w} is weight averaged molecular weight, c is the concentration of lipids, N_{A} is Avogadro's number, and $\Delta\rho$ is the scattering length difference, which can be calculated from the electron number and the molecular weight of the lipid and the solvent. The term $\bar{\upsilon}$ indicates the specific volume of micelles in the solution, which can be determined by the density of the micellar solutions and the solvent (Figure S2).

Multi-angle light scattering coupled with asymmetric flow field flow fractionation (AF4-MALS) measurements. QACaL*n* (10 mg mL^{-1}) was prepared in 50 mM aqueous NaCl. Aliquots (30 μL) of the sample solution were injected into an Eclipse 3+ separation system (Wyatt Technology Europe GmbH, Dernbach, Germany) for asymmetrical flow field flow fractionation (AF4) at 25°C. The output from AF4 was then passed sequentially through a Dawn Heleos II multiangle light-scattering (MALS) detector (Wyatt Technology), UV detector, and an Optilab rEX DSP differential refractive index (RI) detector (Wyatt Technology), operating at a wavelength of 658 nm. A Wyatt channel (Eclipse 3 channel LC) attached to a membrane (polyether sulfone membrane; 1 kDa LC) at the bottom of the channel was used for the measurements. For QACaL3, 4, 5, 6, 7, and 8, the cross-flow and channel-flow rates were fixed at 4.0 and 1.0 mL min^{-1}, respectively. Since QACaL9 forms large self-assembled structures, including cylindrical micelles, the cross-flow was exponentially decreased over time. Detailed experimental procedures are reported elsewhere.[4] The specific refractive index increments ($\partial n/\partial c$) and the extinction coefficients (ε at 270 nm) of the micelles in aqueous solution were determined using a DRM-1021 differential refractometer (Otsuka Electronics, Osaka) and a Jasco V-630 spectrometer, respectively (see Figure S2).

Analytical ultracentrifugation (AUC). Analytical ultracentrifugation of QACaL*n* micelles was performed using a Beckman Optima XL-1 ultracentrifuge at 25 °C. The samples were dissolved in 50 mM aqueous NaCl to be required concentration. The reference cell was filled with the NaCl solution while the sample cell was

filled with the micelle solutions. The rotor speeds were set at 3.0×10^4 rpm. From analyzing the Rayleigh fringe, the apparent weight average molecular weight $M_{w,App}$ and Q (= $M_{w,App}/M_{z,App}$) were determined at each sample concentration, providing the M_w and Q for the samples by extrapolating the concentration to zero. [4]

NMR spectra

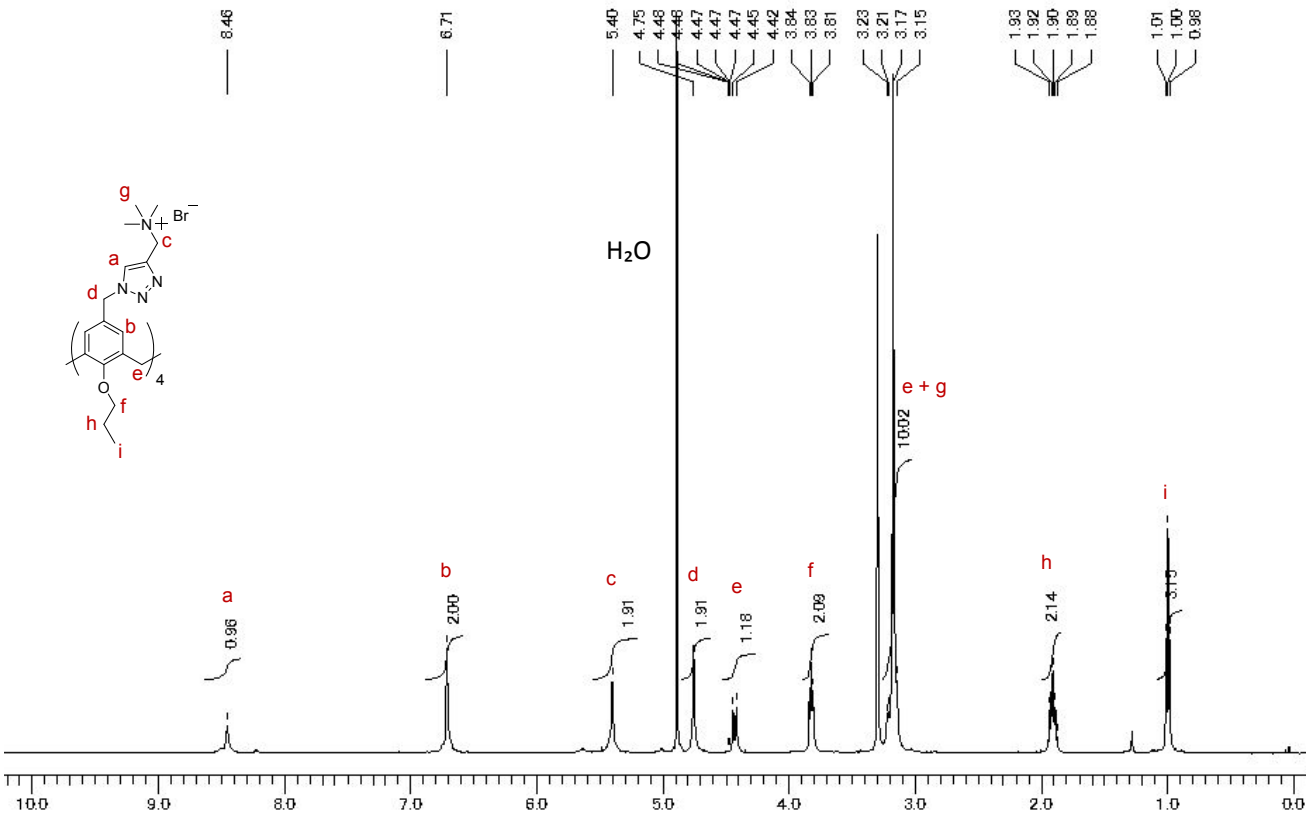

^{1}H-NMR spectrum of compound QACaL3.

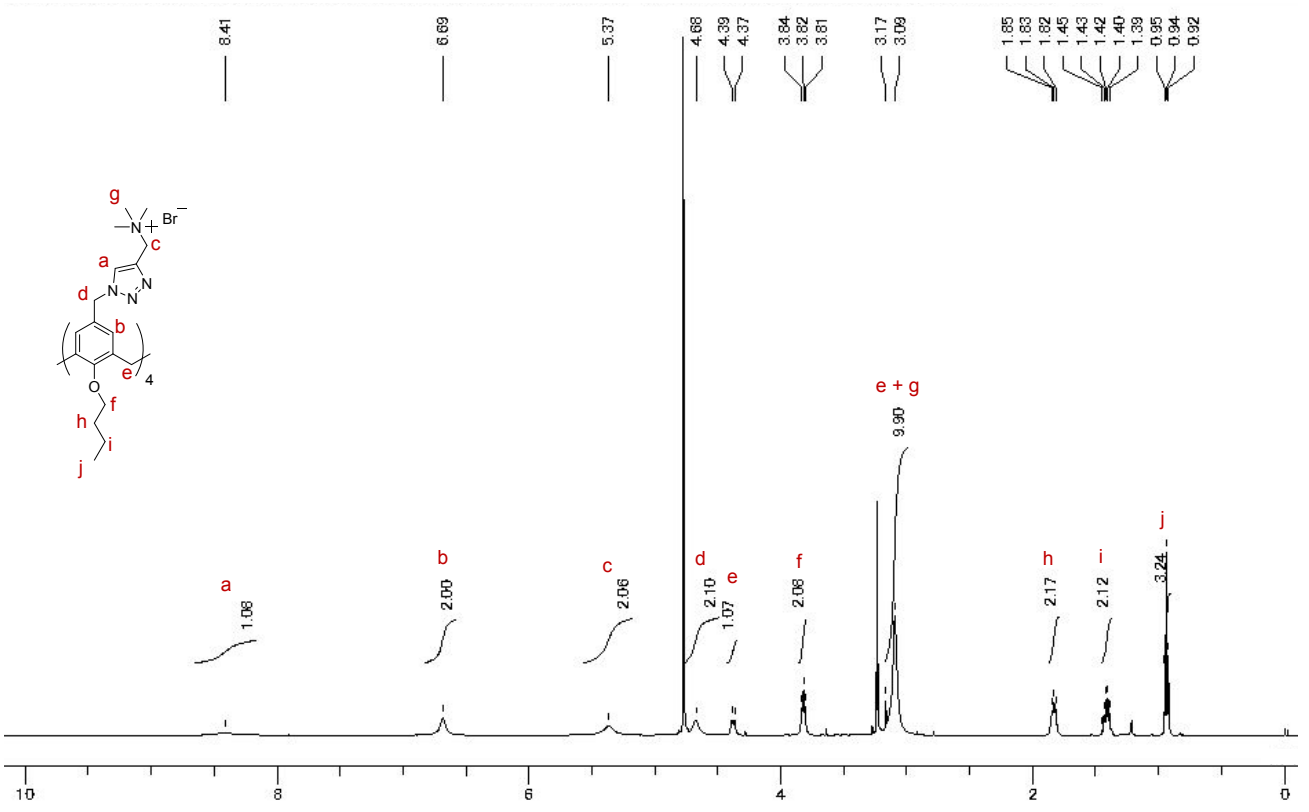

^{1}H-NMR spectrum of compound QACaL4.

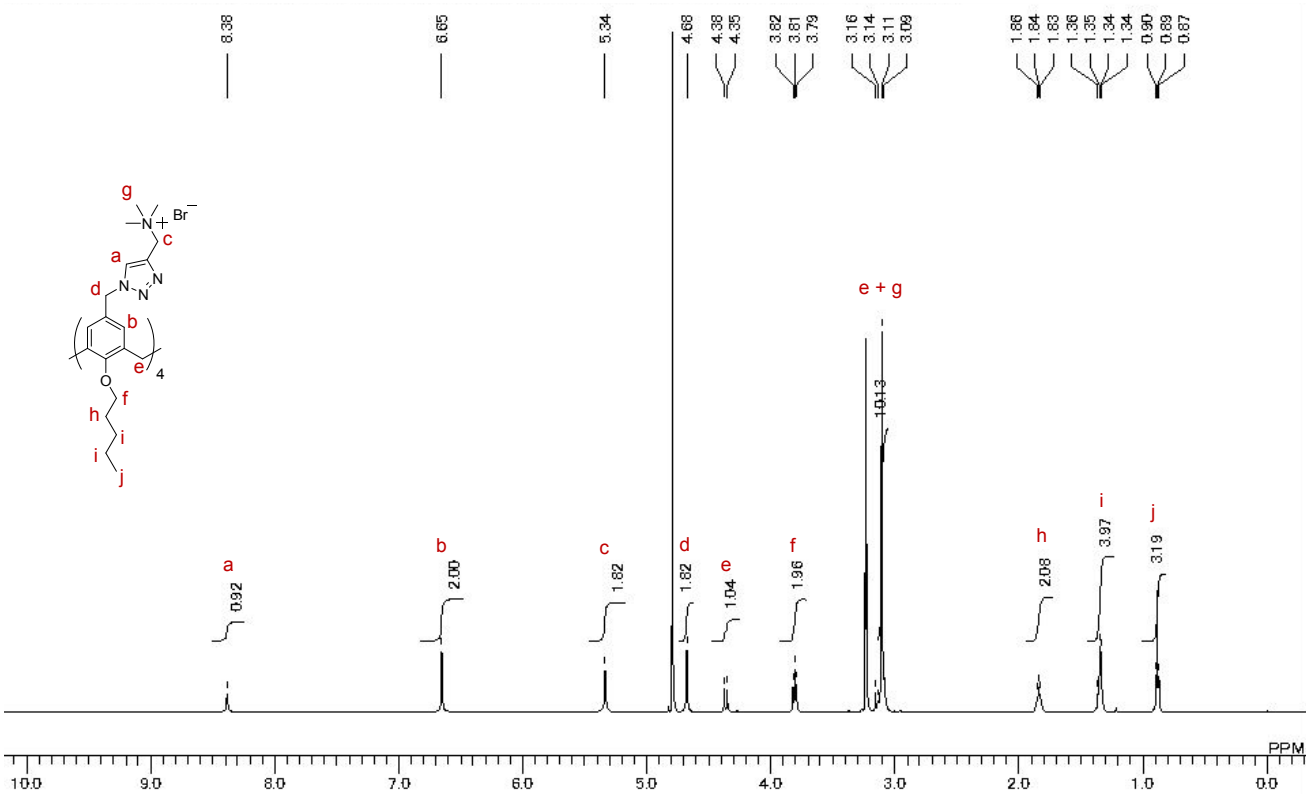

[1]H-NMR spectrum of compound QACaL5.

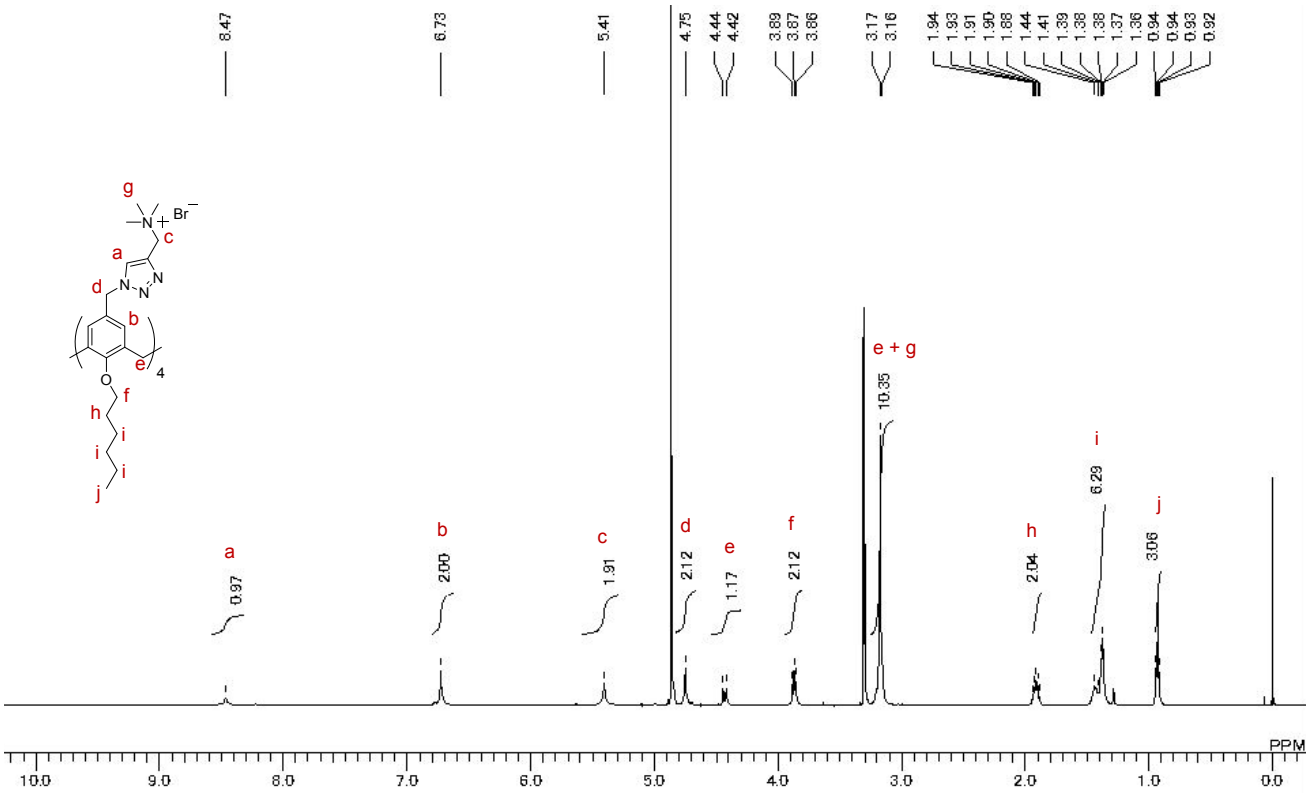

[1]H-NMR spectrum of compound QACaL6.

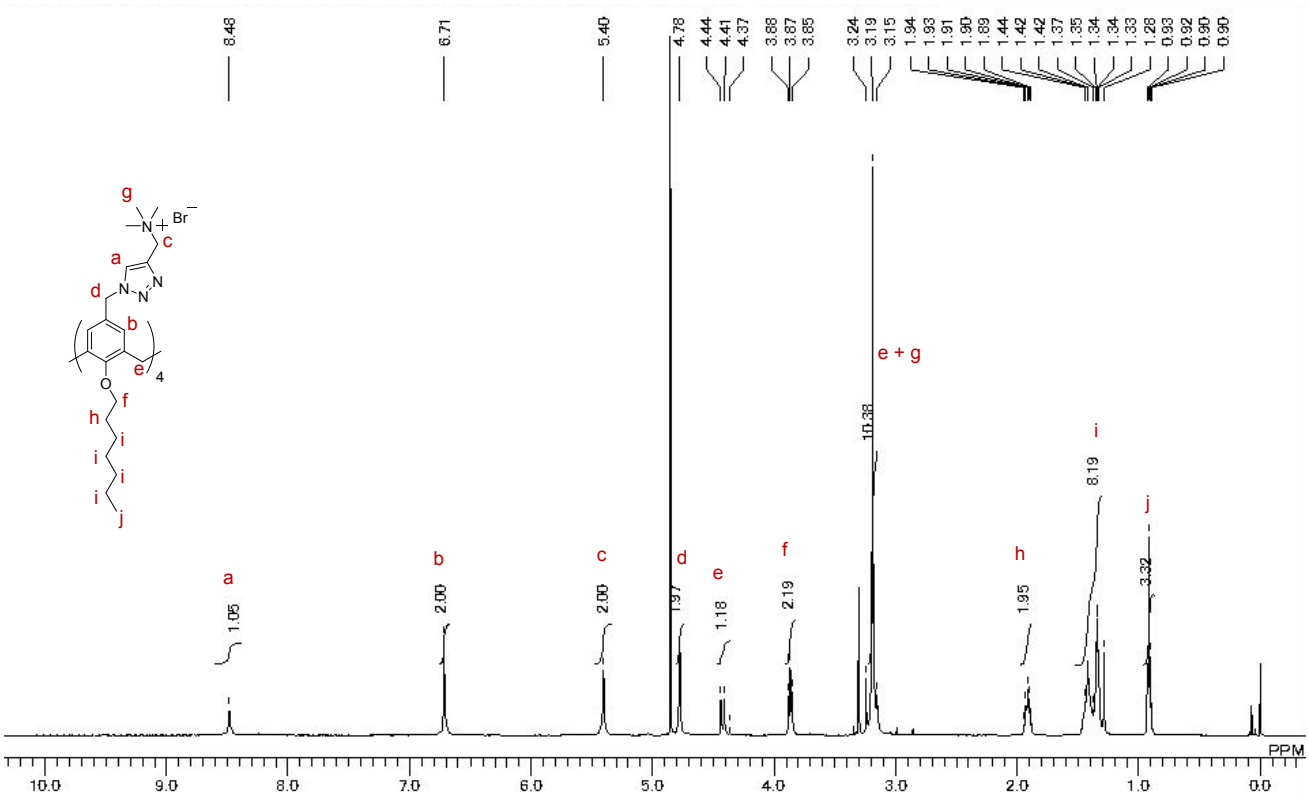

[1]H-NMR spectrum of compound QACaL7.

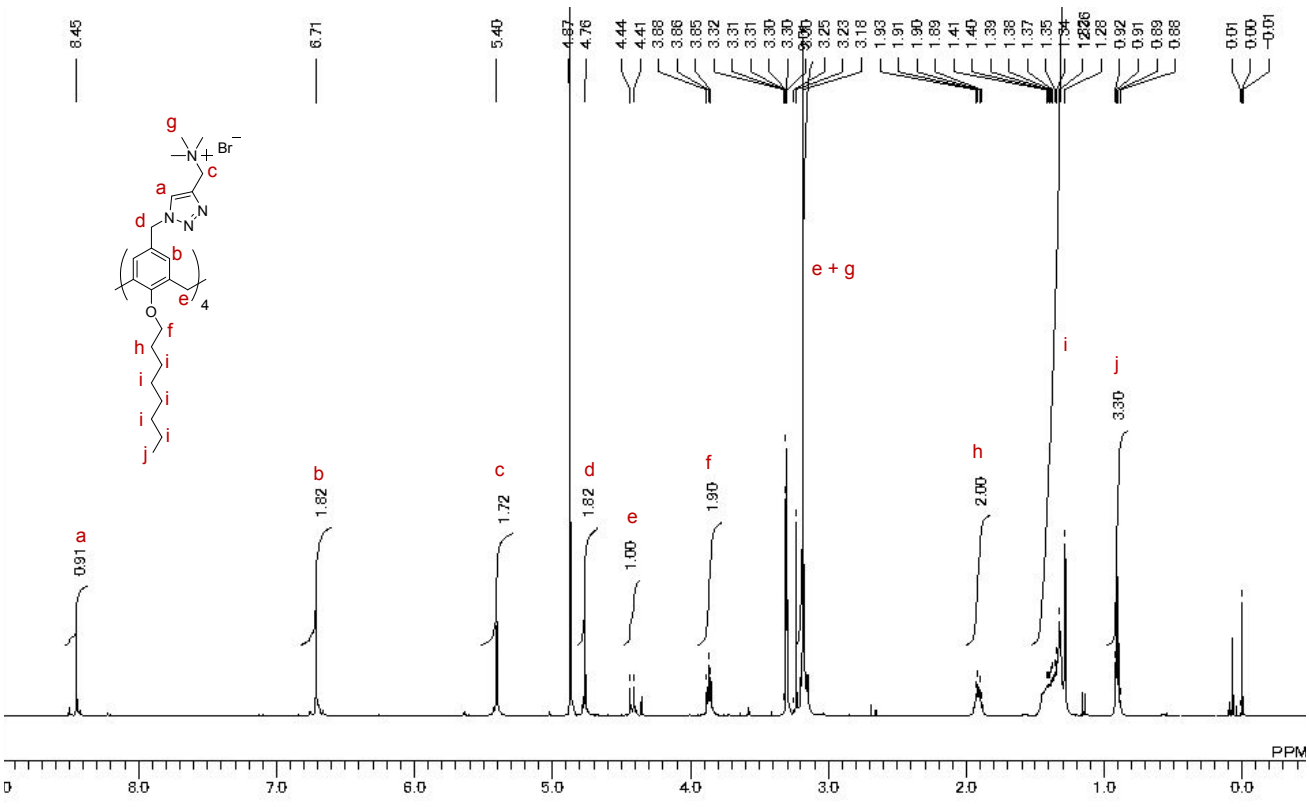

[1]H-NMR spectrum of compound QACaL8.

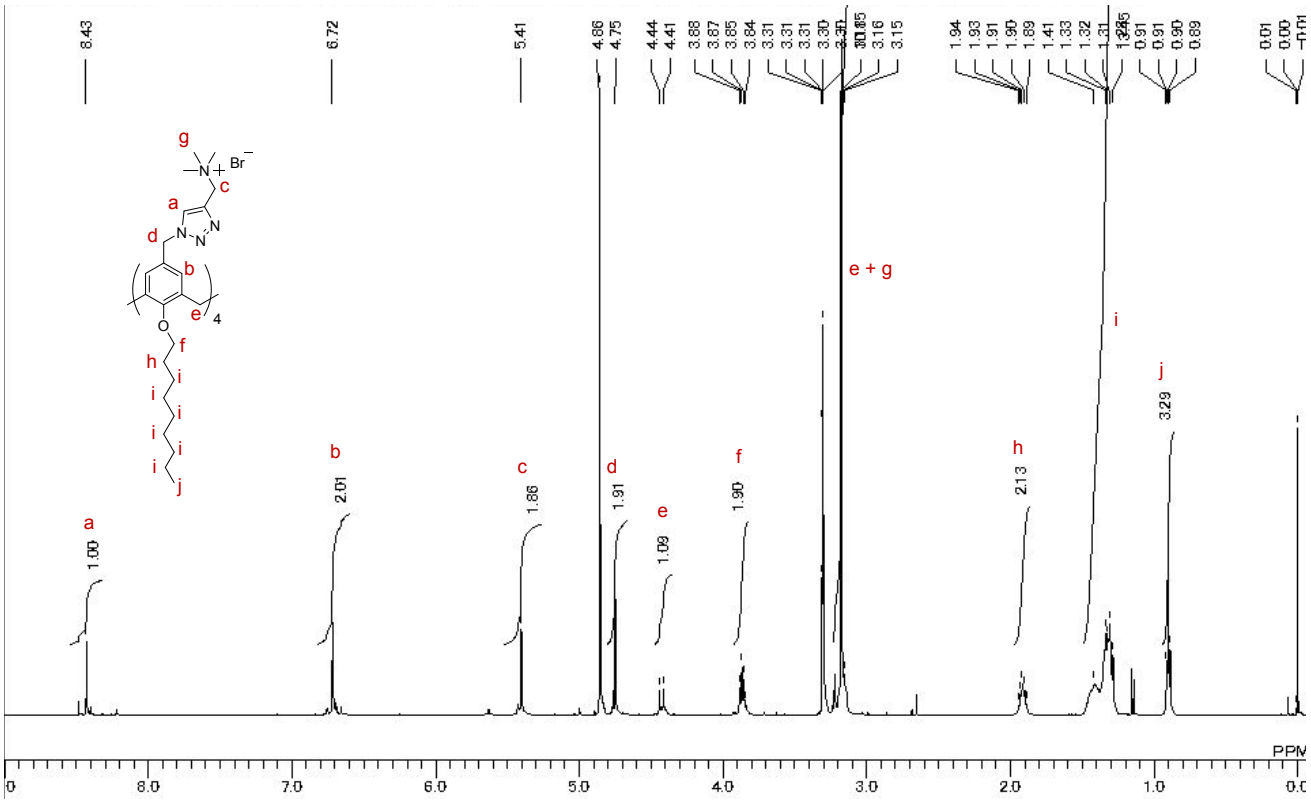

^{1}H-NMR spectrum of compound QACaL9.

Figure S1

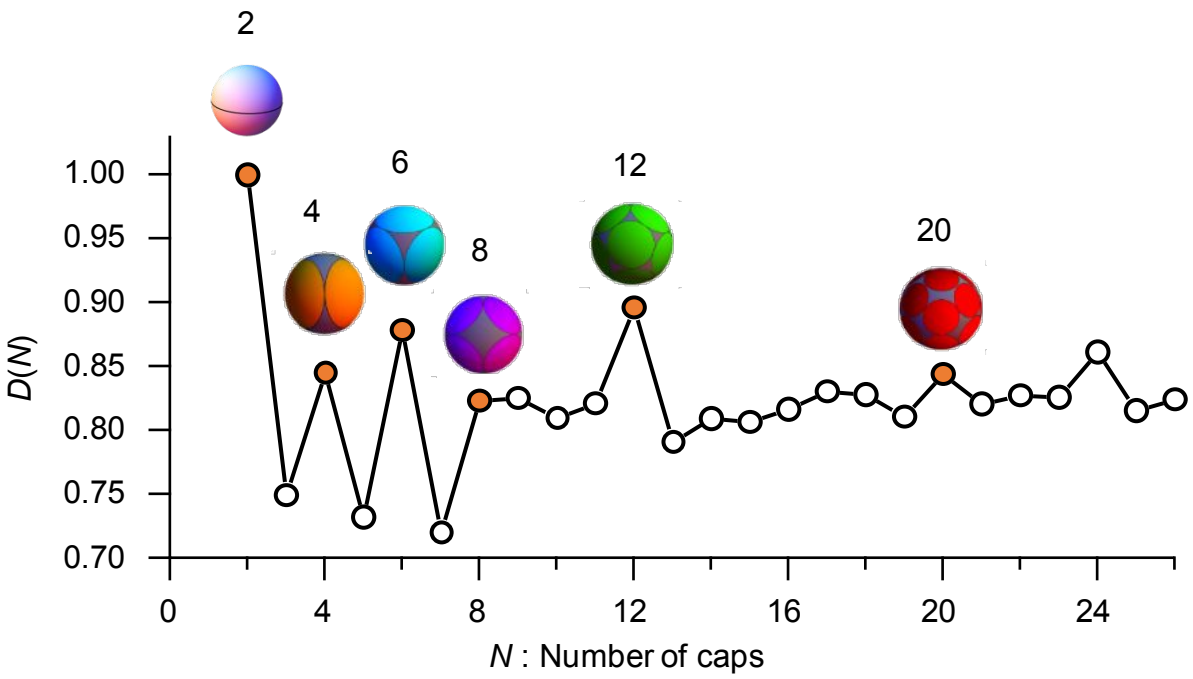

Figure S1. *D*(*N*) for *N* ranging from 2 to 26. Certain numbers produce a local maximum and are identical to the number of the vertices of Platonic solids.

Figure S2

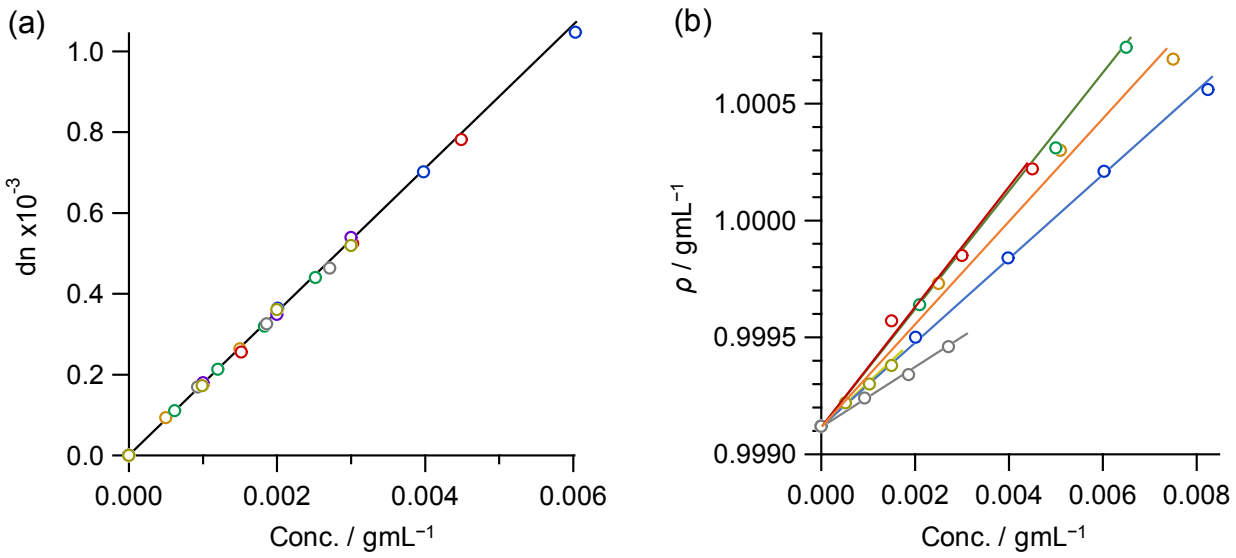

Figure S2. (a) Concentration dependence of refractive index increment and density increment for QACaLn micelles (orange: QACaL3, green: QACaL4, red: QACaL5, yellow: QACaL6, blue: QACaL7, gray: QACaL8, purple: QACaL9) in 50 mM aqueous NaCl.

Figure S3

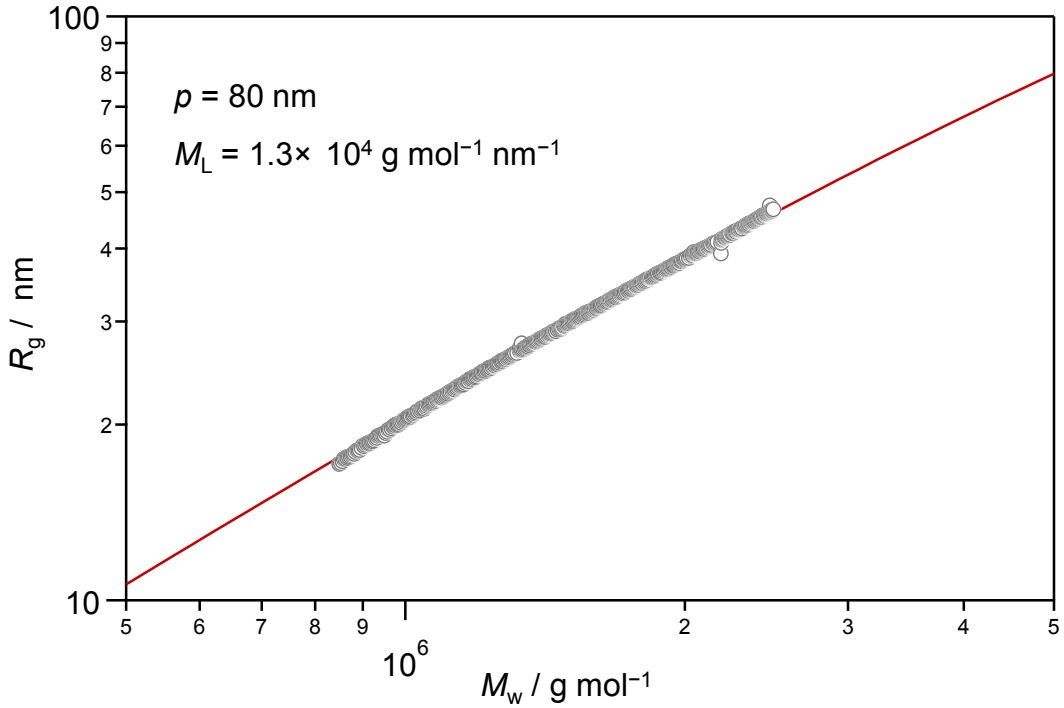

Figure S3. Double logarithmic plot of $\langle S^2 \rangle_z^{1/2}$ vs M_w for QACaL9 micelle in 50 mM NaCl. The solid line are calculated using the Benoit-Doty equation with the indicated parameters.

Figure S4

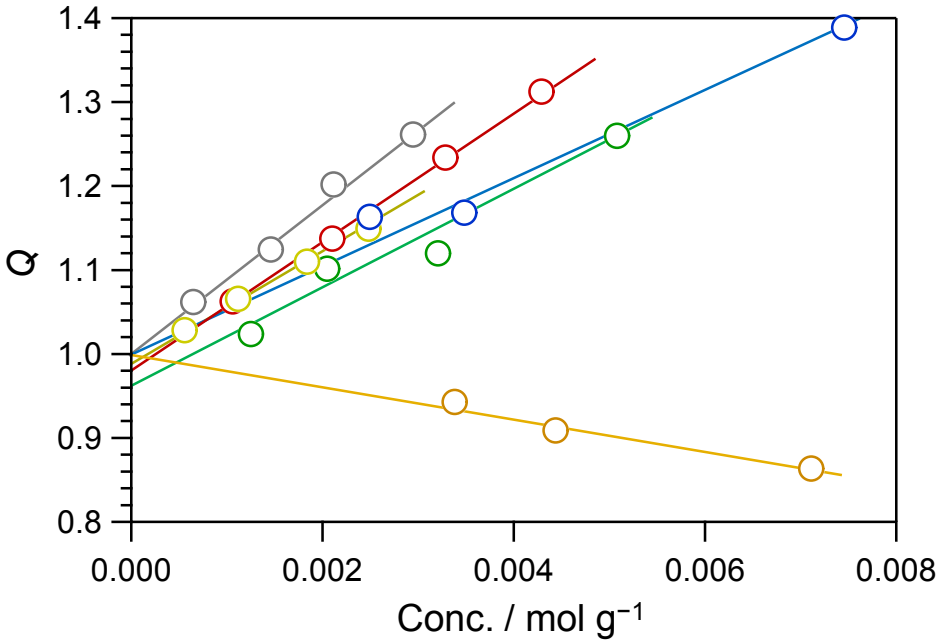

Figure S4. The concentration dependence of Q (= $M_{w,App}/M_{z,App}$) determined by analytical ultracentrifugation measurements for QACaL*n* (orange: QACaL3, green: QACaL4, red: QACaL5, yellow: QACaL6, blue: QACaL7, gray: QACaL8) micelles in 50 mM aqueous NaCl solutions.

Figure S5

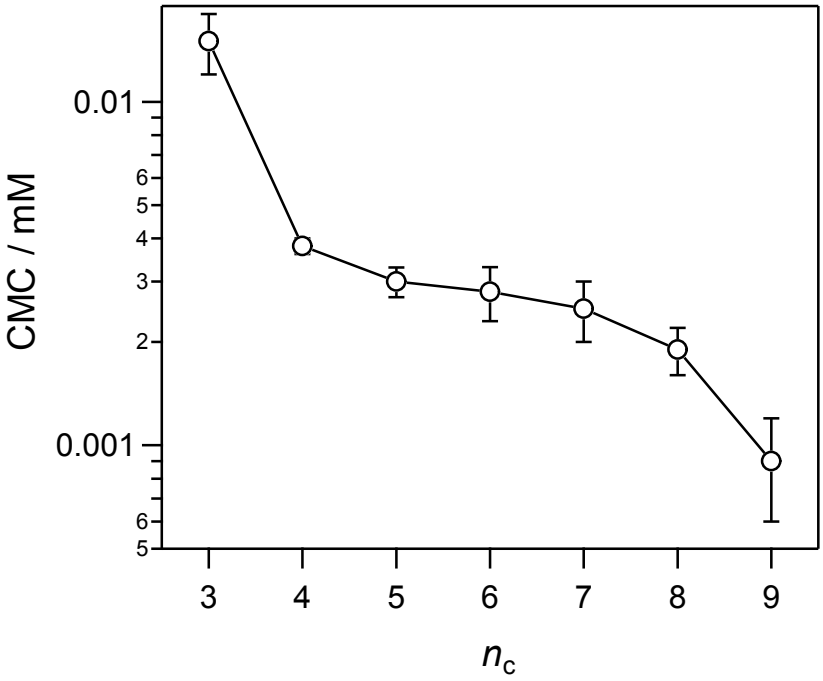

Figure S5. Alkyl chain length (n_c) dependence of critical micelle concetration (CMC)

References

1. S. Fujii, Y. Sanada, T. Nishimura, I. Akiba, K. Sakurai, N. Yagi and E. Mylonas, *Langmuir*, 2012, **28**, 3092-3101.
2. L.A. Feigin, D.I. Svergun, George W. Taylor, Structure analysis by small-angle X-Ray and neutron scattering, Plenum Press, New York, 1987.
3. D. Orthaber, A. Bergmann and O. Glatter, *Journal of Applied Crystallography*, 2000, **33**, 218-225.
4. S. Fujii, J. H. Lee, R. Takahashi and K. Sakurai, *Langmuir*, 2018, **34**, 5072-5078.